

# Immune checkpoint inhibitors modulate the cytotoxic effect of chemotherapy in lung adenocarcinoma cells

MARIKA SAAR<sup>1-3</sup>, DARJA LAVOGINA<sup>3,4</sup>, HELEN LUST<sup>3,4</sup>, HANNES TAMM<sup>5,6</sup> and JANA JAAL<sup>3,7</sup>

<sup>1</sup>Pharmacy Department, Tartu University Hospital, 50406 Tartu; <sup>2</sup>Pharmacy Institute, University of Tartu, 50411 Tartu; <sup>3</sup>Institute of Clinical Medicine, Faculty of Medicine, University of Tartu, 50406 Tartu; <sup>4</sup>Institute of Chemistry, University of Tartu; <sup>5</sup>Institute of Biomedicine and Translational Medicine, Faculty of Medicine, University of Tartu, 50411 Tartu; <sup>6</sup>Pathology Department, Tartu University Hospital; <sup>7</sup>Department of Radiotherapy and Oncological Therapy, Haematology and Oncology Clinic, Tartu University Hospital, 50406 Tartu, Estonia

Received October 26, 2022; Accepted January 25, 2023

DOI: 10.3892/ol.2023.13738

**Abstract.** Immunotherapy using immune checkpoint inhibitors (ICIs) has significantly improved survival in patients with non-small cell lung cancer (NSCLC), and ICIs are increasingly used in combination with cytotoxic treatments, such as chemotherapy. Although combined treatments are more effective, not all patients respond to the therapy; therefore, a detailed understanding of the effect of treatment combinations at the tumour level is needed. The present study aimed to explore whether ICIs could affect the cytotoxic effects of chemotherapy on lung adenocarcinoma cell lines with different PD-L1 expression levels (high, HCC-44; low, A-549). Using the resazurin-based assay, the efficacy of seven chemotherapeutic agents (cisplatin, etoposide, gemcitabine, pemetrexed, vinorelbine, docetaxel and paclitaxel) was compared in the presence or absence of the individually chosen single doses of four ICIs (nivolumab, pembrolizumab, atezolizumab and durvalumab). The results revealed that different ICIs can exhibit either potentiating or depotentiating effects, depending on the chemotherapy agent or lung adenocarcinoma cell line used. Durvalumab was the most promising ICI, which potentiated most chemotherapy agents in both cell lines, especially in the case of high PD-L1 expression. By contrast, nivolumab, exhibited depotentiating trends in several combinations. The immunostaining of  $\gamma$ H2AX in treated cells confirmed that the potentiation of the chemotherapeutic cytotoxicity by durvalumab was at least partially mediated via increased DNA damage; however, this effect was strongly dependent on the chemotherapy agent and cell line used. Our future studies aim to address the specific

mechanisms underlying the observed ICI-induced potentiation or depotentiation.

## Introduction

Lung cancer is the leading cause of cancer-related death and the second most commonly diagnosed cancer worldwide with an estimated 1.8 million deaths and 2.2 million new cases in 2020 (1). For years, standard treatments for patients with advanced metastatic non-small-cell lung cancer (NSCLC) included cytotoxic chemotherapy including platinum (cisplatin or carboplatin) based regimens with third generation cytotoxins (paclitaxel, gemcitabine, docetaxel, and vinorelbine) resulting in a median survival of approximately one year after chemotherapy (2). Until 2008, all platinum doublets used to treat NSCLC were considered equal, since none of the four chemotherapy regimens (cisplatin/paclitaxel, cisplatin/gemcitabine, cisplatin/docetaxel, and carboplatin/paclitaxel) offered a significant advantage over the others (3). Nevertheless, in 2008, it was shown for the first time that overall survival (OS) was significantly superior for cisplatin/pemetrexed vs. cisplatin/gemcitabine in patients with adenocarcinoma histology, while patients with squamous cell histology had a significant improvement in OS with cisplatin/gemcitabine vs. cisplatin/pemetrexed (4). Since then, it is widely accepted that the cytotoxic efficacy of different chemotherapeutics depend on NSCLC histology and treatment should therefore be tailored according to NSCLC subtype.

Recently, immunotherapy with immune checkpoint inhibitors (ICI) has demonstrated durable responses and significantly improved OS in patients with NSCLC. The programmed death receptor 1 (PD-1) and its ligand (PD-L1) are the first introduced checkpoints being targeted in NSCLC, and according to several clinical trials and guidelines, antibodies against PD-1 and PD-L1 have remarkable efficacy both in the first line and second line treatment of metastatic NSCLC, especially in patients with a higher tumour proportion score of PD-L1 (2,5-8). However, despite demonstrated successes, not all patients respond to immunotherapy interventions or progress while on ICI monotherapy. Therefore, most of the recent research is focused on improvement of the activity of

---

*Correspondence to:* Ms. Marika Saar or Professor Jana Jaal, Institute of Clinical Medicine, Faculty of Medicine, University of Tartu, Puusepa 8, 50406 Tartu, Estonia  
E-mail: marika.saar@kliinikum.ee  
E-mail: jana.jaal@kliinikum.ee

**Key words:** lung adenocarcinoma, immune checkpoints, PD-1, PD-L1, immunotherapy

immunotherapies with novel combinations (including cytotoxic agents) together with biomarker optimization. To date, there are few phase III clinical studies that have studied ICI combinations with cytotoxic chemotherapy in NSCLC. For example, in lung adenocarcinoma patients, atezolizumab combination with carboplatin/nab-paclitaxel showed OS of 18.6 months (9), whereas pembrolizumab combination with platinum doublet containing pemetrexed extended OS to 22.0 months (10), showing that even in one histologic subtype, the efficacy of chemotherapeutics and/or ICIs may vary when combined.

It is widely thought that cytotoxic treatment can potentiate immune response while used in combination with immunotherapy (11,12). It has been shown that conventional chemotherapy, apart from the cytotoxic effects, may enhance the activity of immunotherapy by increasing infiltration of CD8 + T cells, maturation of antigen-presenting cells (APCs), and downregulation of regulatory T cells (Tregs) (13). Moreover, recent studies have described the association of non-immune pathways to the outcome of checkpoint blockade (14).

In a previous study we demonstrated a significant positive correlation between the PD-1/PD-L1 axis and tumour cell enzyme DNA-dependent protein kinase (DNA-PK), which is part of a key pathway involved in the repair of cytotoxic cancer therapy-induced damage (15). Therefore, this study aims to explore whether ICIs can affect the cytotoxicity of chemotherapeutics in clinically relevant lung adenocarcinoma cell lines with different PD-L1 expression levels (high: HCC-44, low: A-549) thus specifically addressing the tumour-cell centred effects of combined therapies.

## Materials and methods

**Chemicals and equipment.** Human non-small cell lung carcinoma (adenocarcinoma) cell line HCC-44 and human lung carcinoma (adenocarcinoma) cell line A-549 were from the Leibniz Institute DSMZ (German Collection of Microorganisms and Cell Cultures GmbH). The following therapeutic antibodies were used: durvalumab (Imfinzi 50 mg/ml by Astra Zeneca), atezolizumab (Tecentriq 60 mg/ml by Roche), pembrolizumab (Keytruda 25 mg/ml by Merck Sharp & Dohme), nivolumab (Opdiva 10 mg/ml by Bristol-Myers Squibb Pharma). The following cytotoxic agent stock solutions were used: cisplatin 1 mg/ml, etoposide 20 mg/ml and gemcitabine 100 mg/ml by Accord (Utrecht, Netherlands), docetaxel 1 mg/ml by Accord (Barcelona, Spain) and paclitaxel 6 mg/ml by Fresenius Kabi (Warsaw, Poland). Vinorelbine (tartrate salt) and pemetrexed were from Selleckchem (Munich, Germany); the cell culture grade DMSO was from AppliChem (Darmstadt, Germany).

The solutions and growth medium components for the cell culture were obtained from the following sources: phosphate-buffered saline (PBS), foetal bovine serum (FBS), L-glutamine, Dulbecco's Modified Eagle's medium (DMEM), and Roswell Park Memorial Institute medium (RPMI-1640)-Sigma-Aldrich (Steinheim, Germany); a mixture of penicillin, streptomycin, and amphotericin B-Capricorn (Ebsdorfergrund, Germany). Resazurin and PBS for the viability assay (supplemented with Ca<sup>2+</sup>, Mg<sup>2+</sup>) were from Sigma-Aldrich (St Louis, MO, USA).

The cells were grown at 37°C in 5% CO<sub>2</sub> humidified incubator (Sanyo; Osaka, Japan). For the viability assay, the initial number of cells was counted using TC-10 cell counter (Bio-Rad; Hercules, CA, USA), and the cells were seeded onto transparent 96-well clear flat bottom cell culture plates BioLite 130188 (Thermo Fischer Scientific; Rochester, NY, USA). Fluorescence intensity and absorbance measurements were carried out with Synergy NEO or Cytation 5 multi-mode readers (both from Biotek; Winooski, VT, USA).

The immunohistochemistry (IHC) with PFA-fixed cell pellets and the following light microscopy were carried out according to the previously published protocols (15); 22C3 pharmDx primary antibody was used for staining. The bright-field imaging of IHC samples was carried out using light microscopy by the Pathology Department of Tartu University Hospital according to the protocols used for the analysis of clinical samples (accreditation certificate No M017 by the Estonian Accreditation Centre). Fluorescence microscopy with  $\gamma$ H2AX-immunostained cells was carried out with Cytation 5 multi-mode reader using 20x air objective. For DAPI, 365 nm LED and DAPI filter block were used; for Alexa Fluor® 568, 523 nm LED and RFP filter block were used.

**Treatment of cells prior to IHC.** HCC-44 or A549 cells (passage number below 30) were seeded in growth medium (RPMI-1640 or DMEM supplemented with 10% FBS) onto Petri dishes (1/4 dilution from the confluent Petri) and grown overnight as in culture. Next, treatment with the following compounds or mixtures in usual growth medium was started: 0.49 mg/ml durvalumab, 1  $\mu$ M cisplatin, 5 nM docetaxel, mixture of cisplatin (1  $\mu$ M) and durvalumab (0.49 mg/ml), or mixture of docetaxel (5 nM) and durvalumab (0.49 mg/ml). After 48 h, the treatment mixtures were removed; the cells were rinsed with PBS, detached from the plates using 0.25% trypsin, and then resuspended in the culture medium. After pelleting by centrifugation (5 min at 800 rcf), the cells were treated by the fixation solution and the samples were then treated adhering to the requirements of standard EVS-EN ISO 15189:2012. Two independent IHC experiments were carried out.

**Treatment of cells prior to the viability assay.** The dose-response curves for chemotherapeutic agents in the presence or absence of therapeutic antibodies were performed in the 96-well format. HCC-44 or A549 cells (passage number below 30) were seeded in growth medium (RPMI-1640 or DMEM supplemented with 10% FBS) onto plate at a density of 2,000 cells or 3,500 cells per well, respectively [within the linear range of the method according to the preliminary experiments (16)]. After incubation for 24 h, the growth medium was exchanged, and dilution series of compounds in PBS or PBS supplemented with therapeutic antibodies were added onto the cells (1/10 of the growth medium volume). The following final total concentrations were used: cisplatin and gemcitabine-6-fold dilution starting from 3.3  $\mu$ M; docetaxel and paclitaxel-6-fold dilution starting from 5  $\mu$ M; etoposide-6-fold dilution starting from 34  $\mu$ M; vinorelbine-6-fold dilution starting from 1  $\mu$ M; pemetrexed-6-fold dilution starting from 40  $\mu$ M. The final total concentrations of antibodies were chosen according to the steady-state concentration in serum reported in the literature:

atezolizumab-0.63 mg/ml (17); durvalumab-0.49 mg/ml (18); nivolumab-0.13 mg/ml (19); pembrolizumab-0.09 mg/ml (20). Pure PBS was added to the negative control (100% viability). The final volume per well was 200  $\mu$ l, and the concentration of DMSO in the treated wells was equal to or below 0.1% by volume; on each plate, each concentration of each compound was represented in duplicate. The cells were incubated with compounds in the presence or absence of therapeutic antibodies for 48 h, and the viability assay was then carried out.

**Viability assay.** The growth media was removed from the cells, the cells were rinsed with PBS, and 50  $\mu$ M resazurin solution in PBS (containing  $\text{Ca}^{2+}$  and  $\text{Mg}^{2+}$ ) was applied onto the cells. The plates were placed into a multi-mode reader, and measurements were performed at 30°C in kinetic mode (reading taken every 15 min for 2 h) using the following parameters: (A) fluorescence: excitation 540 nm, emission 590 nm, monochromator, top optics, gain 50; (B) absorbance at 570 and 600 nm, monochromator; read height 8.5 mm.

**$\gamma$ H2AX immunostaining and microscopy.** For immunofluorescence (IF) studies, the cells were grown on 96-well Ibidi black  $\mu$ -plates (ibidi GmbH, Gräfelfing, Germany); the treatment of cells with dilution series of gemcitabine, pemetrexed, cisplatin, docetaxel, paclitaxel, or vinorelbine in the presence or absence of durvalumab was carried out as described above. Following 48 h treatment, the cells were fixed and stained with the rabbit monoclonal IgG against phosphorylated Ser139 of histone H2AX (anti- $\gamma$ H2AX; Sigma-Aldrich, St Louis, MO, USA) and subsequently goat cross-adsorbed antibody against rabbit IgG (H+L) conjugated with Alexa Fluor<sup>®</sup> 568 (Invitrogen; Eugene, OR, USA) as reported previously (21). For the staining of nuclei, 4',6-diamidino-2-phenylindole (DAPI; Invitrogen, Eugene, OR, USA) was used. The imaging was performed in the automated mode; 25 images per well were taken and the DAPI channel was used for autofocusing. The automated image analysis using the Ilastik model and the modified version of MembraneTools module of Aparcium 2.0 software (22) was carried out as reported previously (21).

**Statistical analysis.** For general data analysis, GraphPad Prism 6 (San Diego, CA, USA) and Excel 2016 (Microsoft Office 365; Redmond, WA, USA) were used. In each independent experiment, the fluorescence intensity measured for the replicate treatments was pooled and the data obtained for the negative control was plotted against incubation time with resazurin. One time-point within the duration of data acquisition was chosen where the signal of the negative control stayed in the linear range, and only data measured at this time-point was used for the further analysis.

For normalization of dose-response studies of compounds in the absence of therapeutic antibodies, data obtained for wells treated with PBS (in the absence of compounds; negative control) were considered as 100% viability; in case of dose-response studies of compounds in the presence of antibodies, data obtained for wells treated with PBS supplemented with the corresponding antibodies were considered as 100% viability. For normalization of the effect of the fixed concentrations of antibodies in the absence of chemotherapeutics, data obtained for wells treated with PBS (negative control)

was considered as 100% viability. In all cases, data acquired for the 50  $\mu$ M resazurin solution (in the absence of cells) were considered as 0% viability.

Next, the ratio of absorbance at 570 and 600 nm was calculated for each well. The ratios were analysed analogously to the fluorescence intensity data, and the normalized viability values calculated from the fluorescence intensity and the absorbance measurements were pooled. Finally, data from all independent experiments were pooled ( $n \geq 3$ ).

The pooled normalized viability obtained for serial dilutions was plotted against the concentration of compound in the dilution series and fitted to the logarithmic dose-response function or biphasic function. The statistical significance of difference of calculated negative logarithms of  $\text{IC}_{50}$  values ( $\text{pIC}_{50}$ ) for compounds in the presence vs. absence of therapeutic antibodies was assessed using the one-way ANOVA (95% confidence level) and Dunnett test for multiple comparisons.

For analysis of the IF data, the total intensity of  $\gamma$ H2AX signal in nucleus was plotted against the concentration of a chemotherapeutic agent by pooling data for all nuclei identified from the identically treated cells in all the independent experiments ( $n=3$ ). The normality of data distribution in each condition was tested using the D'Agostino-Pearson test and non-Gaussian distribution was confirmed for most of the tested conditions. For further comparison, the lowest concentration of each chemotherapeutic agent was chosen causing significant elevation of the  $\gamma$ H2AX signal relative to the negative control (PBS-treated cells). For the chosen concentration of each chemotherapeutic agent, the total intensity of  $\gamma$ H2AX signal in nucleus was compared for treatments with and without durvalumab. The statistical significance of difference of calculated negative logarithms of  $\text{IC}_{50}$  values ( $\text{pIC}_{50}$ ) for compounds in the presence vs. absence of ICIs was assessed using the unpaired two-tailed Mann-Whitney test (95% confidence level).

## Results

**Optimization of the viability assay.** Throughout the study, two lung adenocarcinoma cell lines were used, PD-L1 highly positive HCC-44 and weakly positive A-549, to demonstrate the dependence of the observed effects on PD-L1 status (Fig. 1).

For assessment of cell viability, resazurin-based assay was applied. The assay detects changes in fluorescence intensity and the visible light absorption spectrum that are associated with the reduction of resazurin in metabolically active cells. Thus, the higher the fluorescence intensity (excitation 540 nm, emission 590 nm) or 570/600 nm absorption ratio, the more metabolically active cells the given sample contains, and the higher the cellular viability (16). According to our previous study, the resazurin-based assay is superior to the commonly used tetrazolium dye (MTT)-based assay from at least two aspects (16). First, as resazurin and resorufin penetrate cell plasma membrane, measurements with resazurin can be performed in a kinetic mode, without the need for cell lysis after certain incubation time. Second, based on the comparison of the Z'-factors of the either assay, resazurin assay is more sensitive and robust, which is especially important in case if the measured potentiation/depotentiation effects are relatively small.

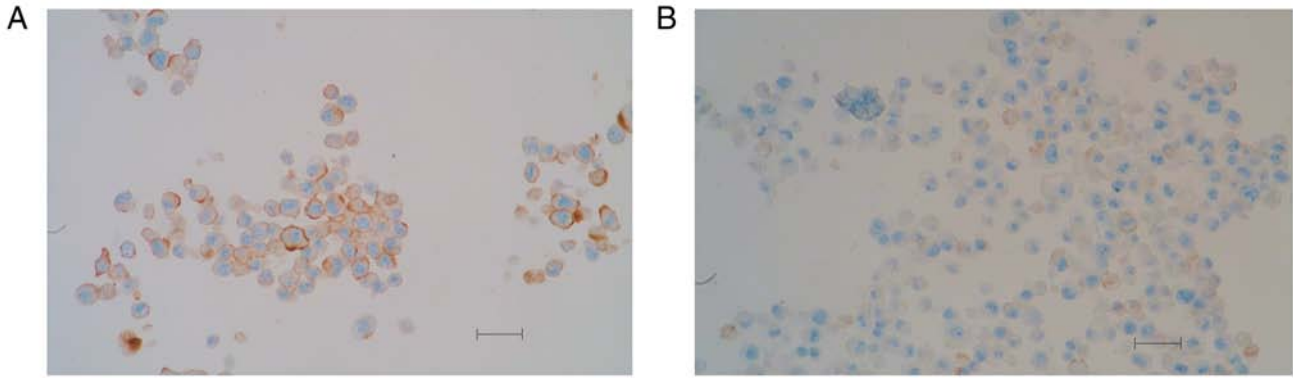


Figure 1. Microscopy images (20x objective) of the immunohistochemically stained (anti-PD-L1) paraffinized cell line pellets. (A) HCC-44; (B) A549. Scale bar (bottom right): 50  $\mu$ m.

Initially, the effect of immune checkpoint inhibitors applied to the individually chosen single doses on viability of the cell lines used in the study was assessed (Fig. 2). The viability was normalized to the negative control (treatment with PBS); normalized mean viability  $\pm$  SEM is shown (for each condition in each cell line,  $n \geq 7$ ). We found that single antibodies had no effect on cell viability in the A549 cell line. In the HCC-44 cell line, only nivolumab had a significant effect ( $P < 0.01$ ), apparently increasing the viability to 110%.

The results regarding the combined antibody effect and chemotherapy in two lung cancer cell lines are summarized in Table I and Fig. 3, as well as in the Figs. S1 and S2.

*Effects of chemotherapeutic agents and mixtures with ICIs on the viability of the HCC-44 cell line.* Using chemotherapeutics only, we found that vinorelbine and docetaxel had the strongest effect on lung adenocarcinoma cells with high levels of PD-L1 expression ( $pIC_{50}$  values of 10.46 and 9.38, respectively), followed by gemcitabine, paclitaxel and pemetrexed (Table I).

In the case of combinations of ICIs with chemotherapeutics, durvalumab potentiated significantly the cytotoxic effect of docetaxel and paclitaxel ( $\Delta pIC_{50}$  values of 0.27 and 0.39, respectively;  $P \leq 0.001$ ), and even more when added to gemcitabine, pemetrexed ( $\Delta pIC_{50}$  values of 0.61 and 0.69, respectively;  $P \leq 0.01$ ) or cisplatin ( $\Delta pIC_{50}$  value of 0.52;  $P \leq 0.001$ ). Only the combination with vinorelbine and etoposide indicated no changes when the antibody was added to chemotherapy. For mixtures containing atezolizumab, significant potentiating effect was seen in the case of docetaxel and paclitaxel ( $\Delta pIC_{50}$  values of 0.41 and 0.75, respectively;  $P \leq 0.001$ ), yet a significant depotentiating effect was observed for vinorelbine ( $\Delta pIC_{50}$  value of -0.90;  $P \leq 0.001$ ). Pembrolizumab potentiated significantly the cytotoxic effect of vinorelbine and docetaxel ( $\Delta pIC_{50}$  values of 0.48 and 0.30, respectively;  $P \leq 0.001$ ), yet no significant changes were detected with other chemotherapy agents. Other combinations where depotentiating effect was observed after adding the antibody were represented by nivolumab with vinorelbine or gemcitabine ( $\Delta pIC_{50}$  values of -1.4 and -0.87, respectively;  $P \leq 0.001$ ) (Fig. 3B-H).

*Effects of chemotherapeutic agents and mixtures with ICIs on the viability of the A549 cell line.* Overall, we found that the effect of chemotherapeutics was weaker in the cell line

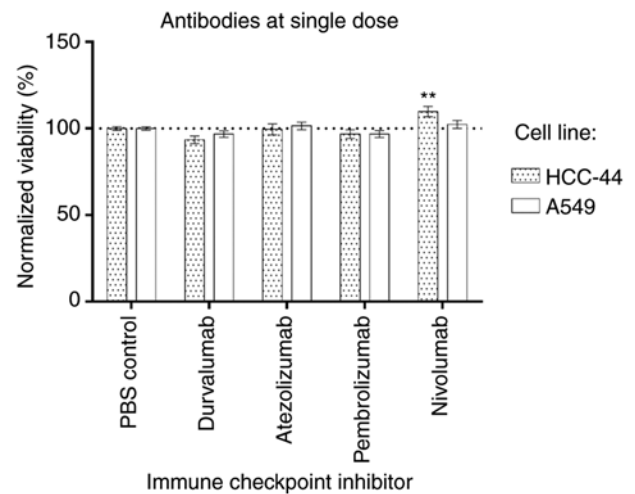


Figure 2. Effect of immune checkpoint inhibitors used at the individually chosen single doses on the viability of the cell lines used in the study. The viability was normalized to the negative control (treatment with PBS); normalized mean viability  $\pm$  SEM is shown (for each condition in each cell line,  $n \geq 7$ ). The statistical significance of difference in cell viability in the presence vs. absence of immune checkpoint inhibitors was assessed using the one-way ANOVA (95% confidence level) and Dunnett test for multiple comparisons (only significant comparisons are shown): \*\* $P < 0.01$  vs. PBS control.

with lower PD-L1 expression, yet most of the observed trends were in line with those measured in the HCC-44 cell line. For instance, vinorelbine and docetaxel affected the viability of lung adenocarcinoma cells the most, with  $pIC_{50}$  values of 8.47 and 8.40 (Table I).

In the case of combinations of ICIs with chemotherapeutics, similar to the HCC-44 cell line, durvalumab potentiated significantly the cytotoxic effect of most chemotherapy agents in A549: e.g. vinorelbine, docetaxel and paclitaxel ( $\Delta pIC_{50}$  values of 0.95, 0.37 and 0.35, respectively;  $P \leq 0.001$ ). The potentiation was also seen in combination with etoposide but to a smaller extent ( $\Delta pIC_{50}$  value of 0.19;  $P < 0.01$ ) as compared to the effect of the durvalumab plus pemetrexed mixture in HCC-44. In contrast to HCC-44 studies, combinations of durvalumab with gemcitabine, pemetrexed and cisplatin indicated no changes when the antibody was added to chemotherapy in A549 cells. Atezolizumab significantly

Table I. Changes in pIC<sub>50</sub> values of chemotherapeutic agents in the presence of therapeutic antibodies.

A, Cell line: HCC-44 (PD-L1 highly positive)					
Compound	pIC <sub>50</sub> ± SEM <sup>a</sup>	ΔpIC <sub>50</sub> in the presence of the ICI <sup>b</sup>			
		Durvalumab	Atezolizumab	Pembrolizumab	Nivolumab
Gemcitabine	8.86±0.09	0.61 <sup>c</sup>	ns	ns	-0.87 <sup>d</sup>
Pemetrexed	7.21±0.10	0.69 <sup>c</sup>	ns	ns	ns
Cisplatin	5.93±0.06	0.52 <sup>d</sup>	ns	ns	ns
Vinorelbine	10.46±0.03	ns	-0.90 <sup>d</sup>	0.48 <sup>d</sup>	-1.4 <sup>d</sup>
Docetaxel	9.38±0.03	0.27 <sup>d</sup>	0.41 <sup>d</sup>	0.30 <sup>d</sup>	0.16 <sup>e</sup>
Paclitaxel	8.60±0.03	0.39 <sup>d</sup>	0.75 <sup>d</sup>	ns	ns
Etoposide	5.88±0.04	ns	ns	ns	ns

B, Cell line: A549 (PD-L1 weakly positive)					
Compound	pIC <sub>50</sub> ± SEM <sup>a</sup>	ΔpIC <sub>50</sub> in the presence of the ICI <sup>b</sup>			
		Durvalumab	Atezolizumab	Pembrolizumab	Nivolumab
Gemcitabine	8.11±0.09	ns	ns	ns	ns
Pemetrexed	5.10±0.09	ns	ns	-0.70 <sup>e</sup>	1.2 <sup>d</sup>
Cisplatin	5.46±0.06	ns	ns	ns	ns
Vinorelbine	8.47±0.04	0.95 <sup>d</sup>	0.22 <sup>e</sup>	1.0 <sup>d</sup>	-0.25 <sup>e</sup>
Docetaxel	8.40±0.04	0.37 <sup>d</sup>	0.31 <sup>d</sup>	0.30 <sup>c</sup>	0.33 <sup>d</sup>
Paclitaxel	7.95±0.03	0.35 <sup>d</sup>	ns	0.18 <sup>e</sup>	ns
Etoposide	5.02±0.03	0.19 <sup>c</sup>	ns	ns	ns

<sup>a</sup>Higher pIC<sub>50</sub> value shows higher potency of compound, SEM, standard error of mean (n≥3). <sup>b</sup>Positive ΔpIC<sub>50</sub> value denotes potentiation of compound's effect on cell viability, whereas negative ΔpIC<sub>50</sub> (coloured in red) denotes depotentiation. The statistical significance of difference in cell viability in the presence vs. absence of ICIs was assessed using the one-way ANOVA (95% confidence level) and Dunnett test for multiple comparisons: <sup>c</sup>P≤0.01; <sup>d</sup>P≤0.001; <sup>e</sup>P≤0.05; ns, not significant relative to the pIC<sub>50</sub> value in the absence of ICIs. ICI, immune checkpoint inhibitor; ΔpIC<sub>50</sub>, shift of negative logarithm of IC<sub>50</sub> value.

potentiated the cytotoxic effect of docetaxel (ΔpIC<sub>50</sub> value of 0.31; P≤0.001) and vinorelbine (ΔpIC<sub>50</sub> value of 0.22; P≤0.05), while no significant changes were detected with other chemotherapy agents. Pembrolizumab had a significant potentiating effect when added to vinorelbine (ΔpIC<sub>50</sub> value of 1.0; P≤0.001) and to a smaller extent in combinations with docetaxel (ΔpIC<sub>50</sub> value of 0.30; P≤0.01) or paclitaxel (ΔpIC<sub>50</sub> value of 0.18; P≤0.05). A depotentiating effect was seen when pembrolizumab was added to pemetrexed (ΔpIC<sub>50</sub> value of -0.70; P≤0.05). Nivolumab had significant potentiating effect when added to pemetrexed and docetaxel (ΔpIC<sub>50</sub> values of 1.2 and 0.33, respectively; P≤0.001), while a depotentiating effect with vinorelbine was observed (ΔpIC<sub>50</sub> value of -0.25; P≤0.05) (Fig. 3B-H).

*Investigation of the mechanisms behind the ICI-mediated potentiation of chemotherapeutic agent cytotoxicity.* In order to clarify the possible molecular mechanisms in which durvalumab could contribute to an increase in the cytotoxicity of chemotherapeutic agents, we performed two additional experiments.

First, to establish whether exposure to chemotherapeutic agents can trigger changes in PD-L1 expression, we carried out PD-L1 staining in both cell lines after 48-h treatment of cells with cisplatin, docetaxel, or the corresponding mixtures with durvalumab. To ensure the survival of a sufficient number of cells for analysis, a single concentration of cisplatin (1 μM) or docetaxel (5 nM) was chosen, corresponding to the IC<sub>50</sub> value of the chemotherapeutic agents in the HCC-44 cell line (which has higher chemosensitivity; Table I). The IHC results are summarized in the Figs. S3 and S4. Overall, no increase in PD-L1 levels was observed for any treatment in either cell line, indicating that the potentiating effects of durvalumab cannot be explained by the increased concentration of the target in cells.

Second, motivated by the previously reported positive correlation between the PD-1/PD-L1 axis and tumour cell DNA-PK expression (15), we examined whether the potentiating effects of ICIs can occur via augmentation of the chemotherapy-induced DNA damage. For that, we carried out immunostaining of a well-recognized DNA damage marker γH2AX in both the HCC-44 and A549 cell lines after 48-h

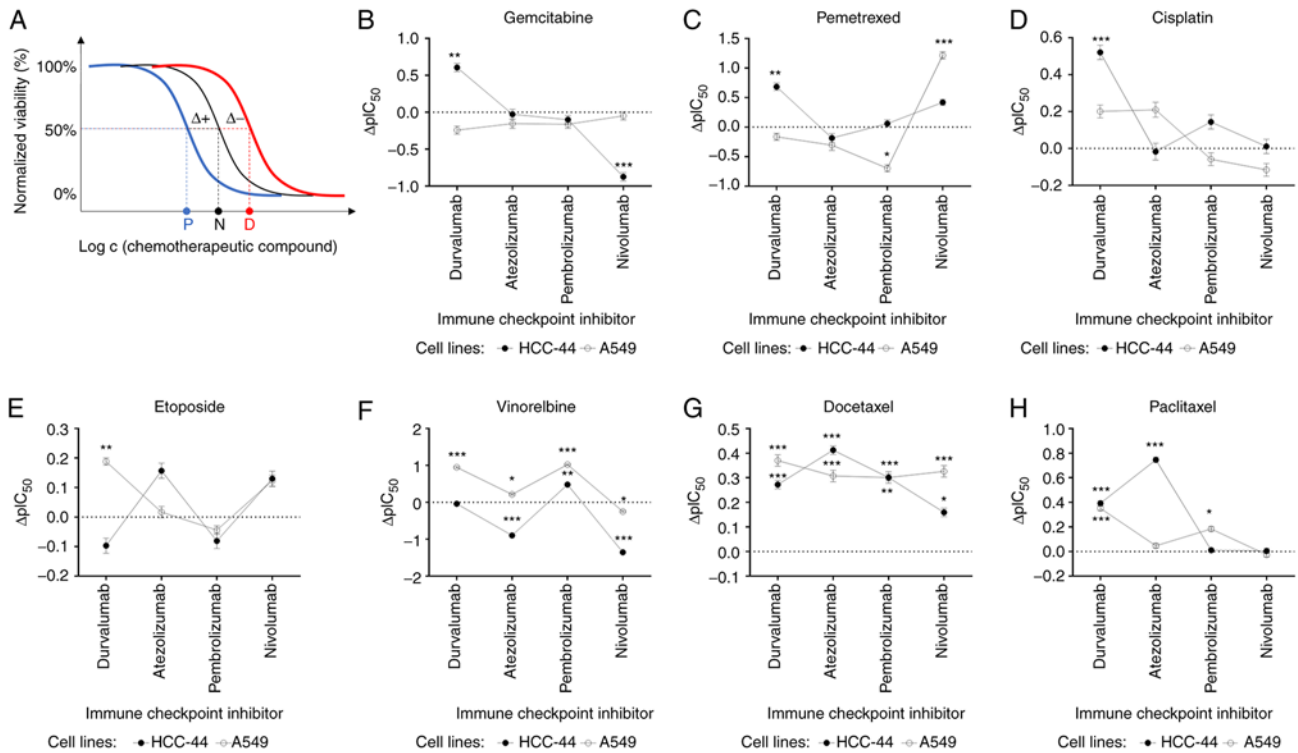


Figure 3. Assessment of the potentiating or depotentiating effect of the ICIs on the viability dose-response curves corresponding to various chemotherapeutic compounds in two cell lines. (A) Principle of the assay: the shift of the normal dose-response curve (black) to lower concentrations (blue) or higher concentrations (red) of a chemotherapeutic compound upon addition of a fixed concentration of an ICI was assessed. The letters P, N, D denote the IC<sub>50</sub> values established for the potentiated, normal, or depotentiated effect; Δ+ indicates shift of IC<sub>50</sub> value in the case of potentiation and Δ- indicates shift of IC<sub>50</sub> value in the case of depotentiation. (B-H) Graphs summarizing the shift of negative logarithms of IC<sub>50</sub> values (ΔpIC<sub>50</sub> ± SEM) for different chemotherapeutic compounds: (B) Gemcitabine, (C) pemetrexed, (D) cisplatin, (E) etoposide, (F) vinorelbine, (G) docetaxel, (H) paclitaxel and ICIs. For each condition in each cell line, n≥3; positive ΔpIC<sub>50</sub> indicates potentiation and negative ΔpIC<sub>50</sub> indicates depotentiation. The statistical significance of difference of calculated pIC<sub>50</sub> values for chemotherapeutic compounds in the presence vs. absence of a therapeutic antibody was assessed using the one-way ANOVA (95% confidence level) and Dunnett test for multiple comparisons (only significant comparisons are shown): \*P<0.05, \*\*P<0.01, \*\*\*P<0.001 relative to the pIC<sub>50</sub> value in the absence of ICIs (indicated in each graph as a dotted line). ICI, immune checkpoint inhibitor.

treatment with chemotherapy agents in the presence or absence of durvalumab. The quantification of total signal intensity of  $\gamma$ H2AX in individual nuclei was carried out using an automated image analysis algorithm. The latter identifies locations of nuclei in images based on the DNA staining in the DAPI channel and quantifies the  $\gamma$ H2AX signal at the same location in the same field of view according to the fluorescently labelled secondary antibody channel. Because such an algorithm is not biased towards the high-intensity nuclei, there is no bottom limit for a detectable  $\gamma$ H2AX signal threshold; hence, the mean  $\gamma$ H2AX signal of the nuclei population can be relatively low. Therefore, given that the chosen validation assay is not suitable for assessment of minor trends, for validation we chose six chemotherapeutic agents for which the ΔpIC<sub>50</sub> value measured in the viability assay was above 0.2 logarithmic units in at least one cell line (Table I).

The cell lines were treated with dilution series of gemcitabine, pemetrexed, cisplatin, docetaxel paclitaxel or vinorelbine in the presence or absence of durvalumab (0.49 mg/ml). The spread of data in each treatment condition is shown in the Figs. S5 and S6. As expected, the profile of the  $\gamma$ H2AX signal changes followed the dose-response curves; in HCC-44, higher levels of DNA damage were observed than in A549, confirming the generally higher chemosensitivity of HCC-44. Consistently with the mechanism of action of the

chemotherapy agents, the highest DNA damage levels were evident for gemcitabine and cisplatin, whereas the cells treated with the microtubule-binding agents (taxanes and vinorelbine) featured the lowest  $\gamma$ H2AX signal.

For quantification of the durvalumab effect, we chose the lowest concentration of the chemotherapy agent from the dose-response curve at which the mean  $\gamma$ H2AX signal was significantly higher than that in the negative control (P<0.05) and compared for this concentration the average  $\gamma$ H2AX signal in the presence vs. absence of durvalumab. Such an approach is more reliable than quantification of the  $\gamma$ H2AX signal at higher concentrations of chemotherapy agents (examples of microscopy images can be seen in the Fig. S7). Specifically, the increase in DNA damage is associated with prevalence of cellular death, and the comparison of dead cell populations in IF methods is problematic due to extensive washing procedures that result in loss of the objects of interest.

The comparisons are summarized in Fig. 4. Overall, according to the increase in the  $\gamma$ H2AX signal in the presence of durvalumab, we could confirm that the potentiating effect of the ICI at least partially occurs via augmentation of the chemotherapy-induced DNA damage in the following treatments: gemcitabine, pemetrexed and paclitaxel in HCC-44, and cisplatin and paclitaxel in A549 (in all cases, P<0.05). In the case of docetaxel treatment of both cell lines, the  $\gamma$ H2AX signal was

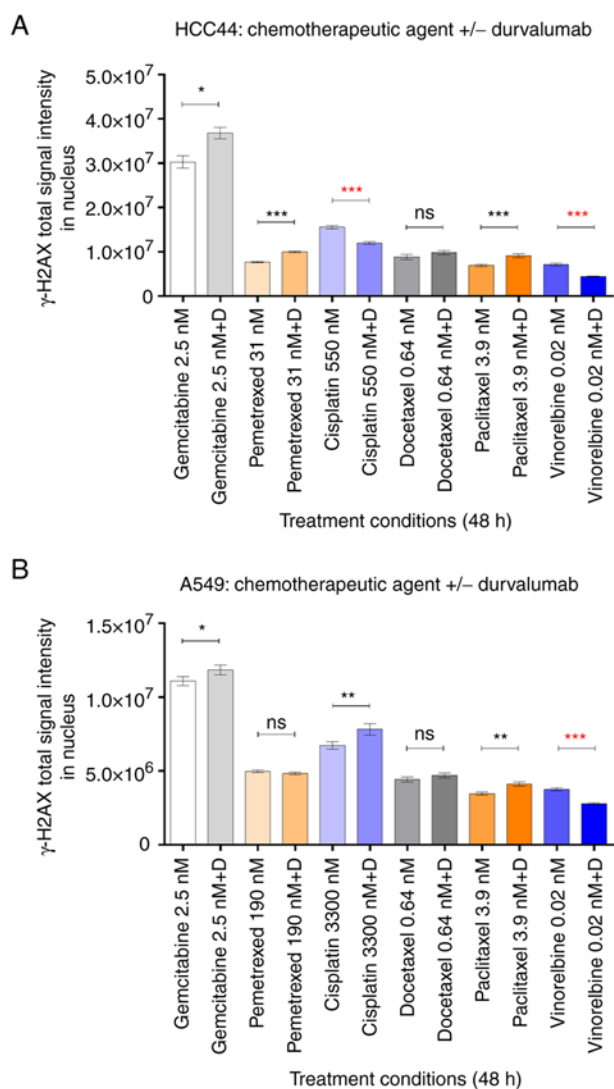


Figure 4. Immunostaining of the DNA damage marker  $\gamma$ H2AX following treatment of lung adenocarcinoma cell lines with various chemotherapeutic agents or their mixtures with durvalumab. (A) HCC-44; (B) A549; the treatment conditions are listed below the graphs (D stands for durvalumab). The mean total signal intensity in individual nuclei  $\pm$  SEM is shown; each graph summarizes data from 6 independent experiments. The statistical significance of signal difference in the presence vs. absence of durvalumab was assessed using the unpaired two-tailed Mann-Whitney test (95% confidence level): \* $P < 0.05$ , \*\* $P < 0.01$ , \*\*\* $P < 0.001$ ; ns, not significant. Red asterisks indicate reduction of  $\gamma$ H2AX levels in the presence of durvalumab. D, durvalumab.

slightly higher in the presence vs. absence of durvalumab, yet the statistical significance of the trend could not be achieved. Interestingly, validation indicated that durvalumab could also somewhat potentiate the DNA-damaging effect of gemcitabine in the A549 cell line ( $P < 0.05$ ), although the corresponding trend was not evident in the viability assay. It is possible that upon prolonged incubation of cells, the trend would also have become evident on the level of cell viability.

It should also be noted that while increase in  $\gamma$ H2AX can be unequivocally correlated to increase in DNA damage and thus interpreted as a mechanism explaining the potentiating effects of the ICI, the decrease in  $\gamma$ H2AX does not indicate depotentiation. Specifically, the decrease in  $\gamma$ H2AX can also occur due to the inability of cells to detect the DNA damage [e.g. as a result of inhibition of ATM kinase that catalyses formation of

$\gamma$ H2AX loci (23)]. Therefore, for treatments such as cisplatin in HCC-44 or vinorelbine in both cell lines where decrease of  $\gamma$ H2AX in the presence of durvalumab was observed, more detailed examination of the molecular mechanisms behind the ICI effect is required.

## Discussion

Currently, immunotherapy with PD-1 and PD-L1 antibodies that enhance the function of anti-tumour T lymphocytes and thereby cause immune activation is in clinical use for the treatment of various tumour types, including lung cancer (2,8,24). However, despite the demonstrated success, especially in patients with a higher tumour proportion score of PD-L1, not all patients respond to immunotherapy interventions or progress while on ICI monotherapy. Therefore, immunotherapy is increasingly used in combination with cytotoxic chemotherapy, thus improving overall survival and prognosis in patients with NSCLC (9,10,12,25).

The combination of ICIs with chemotherapy has been considered a successful strategy due to enhancement of the recognition and elimination of tumour cells by the host immune system and reduction of the immunosuppressive tumour microenvironment (26). It is also believed that cytotoxic treatment can potentiate immune response while used in combination with immunotherapy, and anticancer drugs can induce immunogenic cell death in sensitive tumour cells (11,12,27). Furthermore, chemotherapeutics have different underlying immune modulating molecular mechanisms such as increased T cell recognition (cisplatin, carboplatin), decreased Tregs (paclitaxel), increased T cell infiltrate and antigen presentation (pemetrexed) or enhanced expression of tumour-antigens (gemcitabine), etc (26). However, all the mechanisms underlying synergistic interactions in immunotherapy and chemotherapy combinations are not completely understood and described. We have demonstrated earlier a significant positive correlation between the PD-1/PD-L1 axis and tumour cell enzyme DNA-PK, which is part of a key pathway involved in the repair of cytotoxic cancer therapy induced damage (15). Therefore, to confirm our hypothesis about an alternative role of ICIs in addition to immune activation, we performed the study to test whether ICIs can affect the cytotoxicity of chemotherapeutics. For this, we used clinically relevant lung adenocarcinoma cell lines in the absence of immune cells and tested modulation of the cytotoxic effects of 4 ICIs.

Our study showed that ICIs can indeed modulate cytotoxic effects by potentiating or depotentiating chemotherapy agents. We found that out of all tested ICIs, durvalumab most markedly potentiated cytotoxic effects of chemotherapy agents in both cell lines; however, the effect was slightly stronger in the HCC-44 cell line which has high PD-L1 expression (in 5 out of 7 chemotherapeutics) compared to the cell line A549 with lower levels of PD-L1 (in 4 out of 7 chemotherapeutics) (Fig. 5).

To the best of our knowledge, there are no similar studies that have assessed ICI effects on chemotherapy cytotoxicity. Nevertheless, emerging clinical data indirectly support our findings. For example, compared to chemotherapy alone, the addition of atezolizumab to cisplatin and pemetrexed did not improve OS in lung cancer patients with adenocarcinoma in

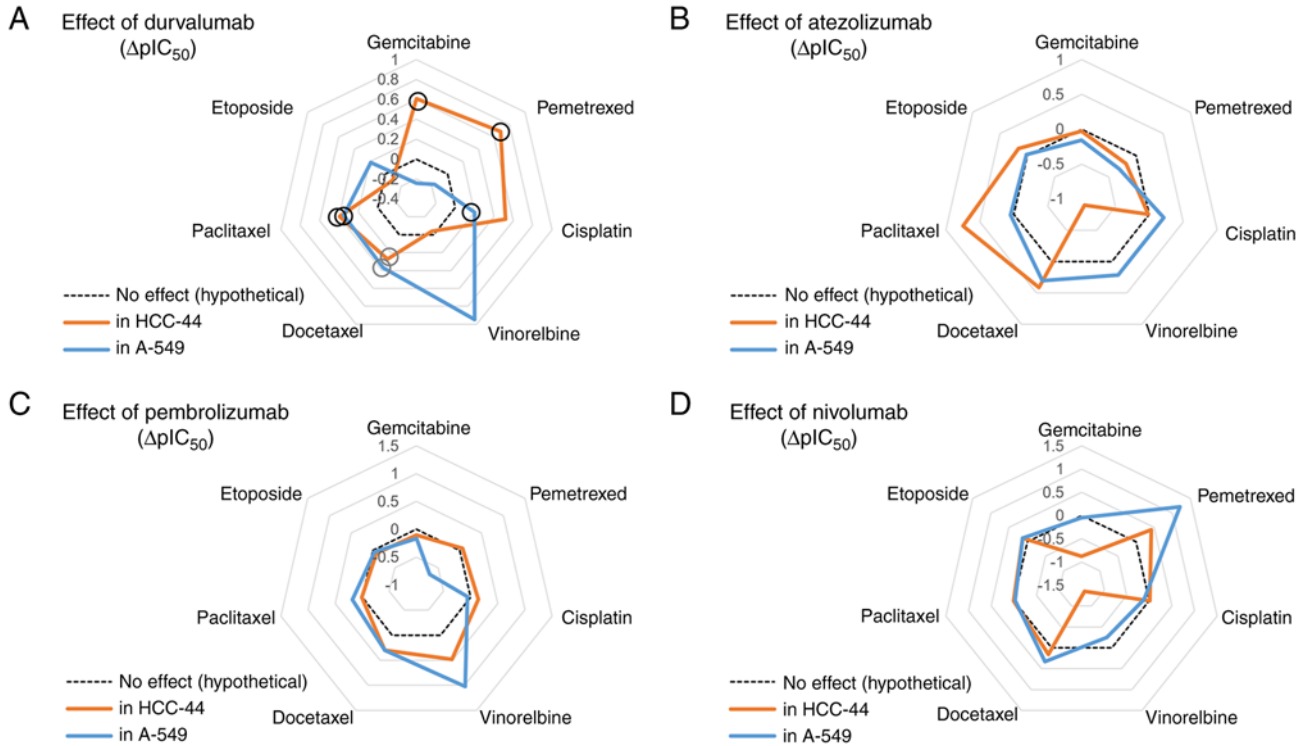


Figure 5. Radar plots summarizing potentiating and depotentiating effects of each immune checkpoint inhibitor. Different chemotherapy agents are listed on the periphery of the plots; the y-axis shows the  $\Delta pIC_{50}$  values in the HCC-44 (orange) and A-549 (blue) cell lines measured using viability assay. The further the data point is located from the centre of the plot, the more potentiating the corresponding antibody is. (A) Durvalumab; (B) atezolizumab; (C) pembrolizumab; (D) nivolumab in combination with the given chemotherapy agent. For better visualization, the thick black line indicates absence of a potentiating or depotentiating effect. In (A), circles indicate the trends confirmed by the validation method ( $\gamma$ H2AX immunostaining); black circles show statistically significant trends and grey circles indicate the trends for which the statistical significance could not be confirmed by validation.  $\Delta pIC_{50}$ , shift of negative logarithm of  $IC_{50}$  value.

the phase 3 IMpower132 study (28). In the context of our data, these findings may also be explained by improper chemotherapy selection since atezolizumab did not potentiate the cytotoxic efficacy of either of the chemotherapeutics used.

Somewhat surprisingly, next to some potentiating actions of atezolizumab, pembrolizumab and nivolumab, these ICIs also exerted depotentiating effects in combination with some chemotherapeutics. Nivolumab had the biggest depotentiating effect, reducing the cytotoxicity of vinorelbine in both cell lines and the effect of gemcitabine only in PD-L1 highly positive cells. The latter was in line with the fact that nivolumab was the only ICI whose monotherapy increased the proliferation of HCC-44 cells compared to the non-treated control. Yet again, unfortunately, there are no studies that can be discussed in comparison to our data. However, in clinical setting, it is well known that in NSCLC patients, hyperprogressive disease can occur presenting as a fast, unexpected, and dramatic increase in tumour burden immediately after exposure to ICIs (29). This paradoxical boost in tumour growth following the use of ICIs has been reported in 4-29% of cancer patients; however, the underlying molecular mechanisms are not fully understood (30). Therefore, our *in vitro* model may serve as an additional tool to study such basic mechanisms.

In clinical practice, it has been shown that PD-L1-positive NSCLC patients might get a higher benefit from PD-1/PD-L1 inhibitors compared to patients with no or very low PD/L1 expression (31). However, PD-L1 expression level may not be the only or the optimal biomarker in predicting and evaluating the efficacy of ICIs: in some studies, patients with negative

and weak expression of PD-L1 did also benefit from immunotherapy or immunotherapy and chemotherapy (6,32,33). The cell lines used in this work were chosen to represent either weak (A549) or strong (HCC-44) PD-L1 positivity (Fig. 1). Interestingly, treatment of cells with durvalumab, cisplatin and docetaxel, or combinations thereof somewhat decreased PD-L1 signal in the cell lines (Figs. S3 and S4). This can be explained by two hypotheses, which need to be validated further. Firstly, at this concentration, both cisplatin, its mixture with durvalumab, and a mixture of docetaxel with durvalumab result in a significant drop in cell viability (Table I). It is well known that the cytotoxic mode of action of cisplatin is mediated by its interaction with DNA to form DNA adducts, which activate several signal transduction pathways, including those involving ATR, p53, p73, and MAPK, and culminate in the activation of apoptosis (34). Also, docetaxel causes apoptosis that follows the cancer cell mitotic arrest (35). As the apoptosis can result in alterations of the cell membrane integrity (36), the latter can trigger the apparent decrease in the PD-L1 membranous signal. Furthermore, in the case of treatment with durvalumab alone or durvalumab-containing mixtures, some degree of competition might occur between the durvalumab and the antibody against PD-L1 used for IHC, which would manifest as an apparent decrease in the IHC-detected PD-L1 signal. Still, the difference in PD-L1 status between the cell lines used was overall conserved after the treatment of cells. Given the fact that potentiation of certain chemotherapeutic agents by ICIs was evident in the A549 cell line according to both the viability assay (Table I) and the IF assay (Fig. 4),



our study points to the fact that both adenocarcinoma subtypes may potentially benefit from the ICI and chemotherapy combinations.

In terms of immunomodulatory effects, previous *in vitro* studies have shown that PD-L1 antibodies are superior to the PD-1 antibodies in reverting PD-1/PD-L1 signalling, whereas pembrolizumab is a slightly more effective PD-1 blocker than nivolumab (37). Our *in vitro* study in clinically relevant lung adenocarcinoma cell lines showed heterogeneous modulation of the cytotoxic effects of ICI-chemotherapy combinations that depended on the ICI and chemotherapeutic drugs used and the PD-L1 status of cells, pointing toward the need for careful selection of drugs into combinations. The variations in results for combinations of different ICIs with chemotherapeutics could be explained by differences in affecting receptors, epitopes, and binding sites of ICIs. Nivolumab and pembrolizumab disrupt the PD-1 immune checkpoint pathway through blockade of PD-1 receptors on T lymphocytes, while durvalumab and atezolizumab target PD-L1, thus improving the effector activity of anti-tumour T cells (24). Moreover, PD-1 antibodies are IgG4, whereas the PD-L1 antibodies harbour unmodified (avelumab) or modified IgG1 Fc sequences (durvalumab and atezolizumab) (37). Also, although durvalumab and atezolizumab are both PD-L1 antibodies, those bind to PD-L1 via different binding sites (38). How much and in which way these differences in ICI binding mechanisms affect cytotoxic effects in combinations with chemotherapeutics remains to be discovered.

Recent clinical data by Banchereau *et al* revealed that DNA damage repair genes are associated with good ICI response in PD-L1-positive tumours (14). This is in line with our previous findings that showed a similar link between PD-1/PD-L1 axis and tumour cell DNA repair enzyme DNA-PK (15). Within this work, we confirmed that potentiation of gemcitabine, pemetrexed and taxane cytotoxicity can be explained by augmentation of the DNA damage in the presence of the ICI (Fig. 4). However, the levels of the damage marker  $\gamma$ H2AX following treatment with cisplatin in the HCC-44 cell line or vinorelbine in both cell lines were significantly reduced in the presence of durvalumab, urging the need to explore the molecular pathways behind potentiation in greater detail. For instance, given the fact that the CDK4/6 natural inhibitor CDKN2A has been reported as a significant transcriptional correlate of ICI response (14), and that cisplatin is known to cause cell cycle arrest (39), the targets related to the cell cycle might be of special interest. In our further studies, we will address the specific mechanisms behind the observed potentiating or depotentiating effects of ICIs on chemotherapy cytotoxicity using the large-scale proteomics approach.

This report has several limitations, including the *in vitro* experimental setting and the lack of data on PD-L1 negative adenocarcinoma cells. Nevertheless, we have used clinically relevant human cell lines that represent 2/3 of lung adenocarcinoma patients (PD-L1 highly and PD-L1 weakly positive subgroups). Moreover, we have tested and compared 4 ICIs, based on patients' steady-state serum concentrations after clinically approved antibody dosages, making our data more valuable. The use of preclinical animal models for evaluation of the potentiating or depotentiating effects of ICI and chemotherapy combinations remains an open challenge. Given

our intention to examine specifically the effects of ICIs on the level of tumour cells and not the immune system, relevant animal models are currently not available—since even the most appropriate human immune system-modelling mice still show infiltrating T-cells and inflammatory signature that would not allow to distinguish between the immune-related vs. direct effects of therapy on tumour cells (40).

Despite the aforementioned limitations, we have shown for the first time that ICIs can directly modulate cytotoxic effects by either potentiating or depotentiating chemotherapy agents used in lung adenocarcinoma cell lines. Durvalumab was the most promising ICI, potentiating most chemotherapy agents in both cell lines, especially in the presence of high PD-L1 expression. Nivolumab, on the other hand, showed depotentiating trends in several combinations, pointing toward the need for careful selection of chemotherapeutics into possible combinations with ICIs. Out of 7 tested chemotherapeutics, only docetaxel showed increased cytotoxicity in combination with all ICIs irrespective of the strength of PD-L1 positivity in lung adenocarcinoma cells. Whether it holds true in clinical setting has to be validated in prospective clinical trials.

#### Acknowledgements

Not applicable.

#### Funding

The study was supported by internal financing from the Institute of Clinical Medicine, University of Tartu, Estonia (2019-2022; PI: Dr Jana Jaal).

#### Availability of data and materials

The datasets generated and/or analyzed during the current study are available in the FigShare repository, <https://doi.org/10.6084/m9.figshare.17099042>. All other data are available from the corresponding author on reasonable request.

#### Authors' contributions

MS, DL and JJ conceptualized and designed the study, analysed and interpreted the data, and drafted and revised the manuscript. HL carried out work in cell culture, DL performed viability measurements and HT performed IHC studies. MS, DL and JJ confirm the authenticity of all the raw data. All authors read and approved the final manuscript.

#### Ethics approval and consent to participate

Not applicable.

#### Patient consent for publication

Not applicable.

#### Competing interests

MS, DL, HL, and HT declare no competing interests. JJ is an advisory board member for AstraZeneca, Amgen, Johnson &

Johnson and MSD and has received research funding from AstraZeneca.

## References

- Sung H, Ferlay J, Siegel RL, Laversanne M, Soerjomataram I, Jemal A and Bray F: Global cancer statistics 2020: GLOBOCAN estimates of incidence and mortality worldwide for 36 cancers in 185 countries. *CA Cancer J Clin* 71: 209-249, 2021.
- Planchard D, Popat S, Kerr K, Novello S, Smit EF, Faivre-Finn C, Mok TS, Reck M, Van Schil PE, Hellmann MD, *et al*: Metastatic non-small cell lung cancer: ESMO clinical practice guidelines for diagnosis, treatment and follow-up. *Ann Oncol* 29 (Suppl 4): iv192-iv237, 2018.
- Schiller JH, Harrington D, Belani CP, Langer C, Sandler A, Krook J, Zhu J and Johnson DH; Eastern Cooperative Oncology Group: Comparison of four chemotherapy regimens for advanced non-small-cell lung cancer. *N Engl J Med* 346: 92-98, 2002.
- Scagliotti GV, Parikh P, von Pawel J, Biesma B, Vansteenkiste J, Manegold C, Serwatowski P, Gatzemeier U, Digumarti R, Zukin M, *et al*: Phase III study comparing cisplatin plus gemcitabine with cisplatin plus pemetrexed in chemotherapy-naïve patients with advanced-stage non-small-cell lung cancer. *J Clin Oncol* 26: 3543-3551, 2008.
- Brahmer JR, Rodríguez-Abreu D, Robinson AG, Hui R, Csőszi T, Fülöp A, Gottfried M, Peled N, Tafreshi A, Cuffe S, *et al*: Health-related quality-of-life results for pembrolizumab versus chemotherapy in advanced, PD-L1-positive NSCLC (KEYNOTE-024): A multicentre, international, randomised, open-label phase 3 trial. *Lancet Oncol* 18: 1600-1609, 2017.
- Reck M, Rodríguez-Abreu D, Robinson AG, Hui R, Csőszi T, Fülöp A, Gottfried M, Peled N, Tafreshi A, Cuffe S, *et al*: Updated analysis of KEYNOTE-024: Pembrolizumab versus platinum-based chemotherapy for advanced non-small-cell lung cancer with PD-L1 tumor proportion score of 50% or greater. *J Clin Oncol* 37: 537-546, 2019.
- Mok TSK, Wu YL, Kudaba I, Kowalski DM, Cho BC, Turna HZ, Castro G Jr, Srimuninnimit V, Laktionov KK, Bondarenko I, *et al*: Pembrolizumab versus chemotherapy for previously untreated, PD-L1-expressing, locally advanced or metastatic non-small-cell lung cancer (KEYNOTE-042): A randomised, open-label, controlled, phase 3 trial. *Lancet* 393: 1819-1830, 2019.
- Incorvaia L, Fanale D, Badalamenti G, Barraco N, Bono M, Corsini LR, Galvano A, Gristina V, Listì A, Vieni S, *et al*: Programmed death ligand 1 (PD-L1) as a predictive biomarker for pembrolizumab therapy in patients with advanced non-small-cell lung cancer (NSCLC). *Adv Ther* 36: 2600-2617, 2019.
- West H, McCleod M, Hussein M, Morabito A, Rittmeyer A, Conter HJ, Kopp HG, Daniel D, McCune S, Mekhail T, *et al*: Atezolizumab in combination with carboplatin plus nab-paclitaxel chemotherapy compared with chemotherapy alone as first-line treatment for metastatic non-squamous non-small-cell lung cancer (IMpower130): A multicentre, randomised, open-label, phase 3 trial. *Lancet Oncol* 20: 924-937, 2019.
- Gadgeel S, Rodríguez-Abreu D, Speranza G, Esteban E, Felip E, Dómine M, Hui R, Hochmair MJ, Clingan P, Powell SF, *et al*: Updated analysis from KEYNOTE-189: Pembrolizumab or placebo plus pemetrexed and platinum for previously untreated metastatic nonsquamous non-small-cell lung cancer. *J Clin Oncol* 38: 1505-1517, 2020.
- Hadash-Bengad R, Hajaj E, Klein S, Merims S, Frank S, Eisenberg G, Yakobson A, Orevi M, Caplan N, Peretz T, *et al*: Immunotherapy potentiates the effect of chemotherapy in metastatic melanoma—a retrospective study. *Front Oncol* 10: 70, 2020.
- Judd J and Borghaei H: Combining immunotherapy and chemotherapy for non-small cell lung cancer. *Thorac Surg Clin* 30: 199-206, 2020.
- Tseng CW, Hung CF, Alvarez RD, Trimble C, Huh WK, Kim D, Chuang CM, Lin CT, Tsai YC, He L, *et al*: Pretreatment with cisplatin enhances E7-specific CD8+ T-cell-mediated antitumor immunity induced by DNA vaccination. *Clin Cancer Res* 14: 3185-3192, 2008.
- Banchereau R, Leng N, Zill O, Sokol E, Liu G, Pavlick D, Maund S, Liu LF, Kadel E III, Baldwin N, *et al*: Molecular determinants of response to PD-L1 blockade across tumor types. *Nat Commun* 12: 3969, 2021.
- Saar M, Narits J, Mägi L, Aaspõllu H, Vapper A, Kase M, Minajeva A, Vooder T, Tamm H, Buldakov M, *et al*: Expression of immune checkpoint PD-1 in non-small cell lung cancer is associated with tumor cell DNA-dependent protein kinase. *Mol Clin Oncol* 15: 211, 2021.
- Lavogina D, Lust H, Tahk MJ, Laasfeld T, Vellama H, Nasirova N, Vardja M, Eskla KL, Salumets A, Rincken A and Jaal J: Revisiting the resazurin-based sensing of cellular viability: Widening the application horizon. *Biosensors (Basel)* 12: 196, 2022.
- European Medicines Agency: Tecentriq. <https://www.ema.europa.eu/en/medicines/human/EPAR/tecentriq>. Accessed November 11, 2021.
- European Medicines Agency: Imfinzi. <https://www.ema.europa.eu/en/medicines/human/EPAR/imfinzi>. Accessed November 11, 2021.
- European Medicines Agency: Opdivo. <https://www.ema.europa.eu/en/medicines/human/EPAR/opdivo>. Accessed November 11, 2021.
- European Medicines Agency: Keytruda. <https://www.ema.europa.eu/en/medicines/human/EPAR/keytruda>. Accessed November 11, 2021.
- Lavogina D, Laasfeld T, Vardja M, Lust H and Jaal J: Viability fingerprint of glioblastoma cell lines: Roles of mitotic, proliferative, and epigenetic targets. *Sci Rep* 11: 20338, 2021.
- Aparecium. GPCR Workgroup UT; <https://gpcr.ut.ee/aparecium.html> (Accessed on December 19, 2022).
- Noubissi FK, McBride AA, Leppert HG, Millet LJ, Wang X and Davern SM: Detection and quantification of  $\gamma$ -H2AX using a dissociation enhanced lanthanide fluorescence immunoassay. *Sci Rep* 11: 8945, 2021.
- Hargadon KM, Johnson CE and Williams CJ: Immune checkpoint blockade therapy for cancer: An overview of FDA-approved immune checkpoint inhibitors. *Int Immunopharmacol* 62: 29-39, 2018.
- Paz-Ares L, Luft A, Vicente D, Tafreshi A, Gümüş M, Mazières J, Hermes B, Çay Şenler F, Csőszi T, Fülöp A, *et al*: Pembrolizumab plus chemotherapy for squamous non-small-cell lung cancer. *N Engl J Med* 379: 2040-2051, 2018.
- Leonetti A, Wever B, Mazzaschi G, Assaraf YG, Rolfo C, Quaini F, Tiseo M and Giovannetti E: Molecular basis and rationale for combining immune checkpoint inhibitors with chemotherapy in non-small cell lung cancer. *Drug Resist Updat* 46: 100644, 2019.
- Fucikova J, Kralikova P, Fialova A, Brtnicky T, Rob L, Bartunkova J and Spisek R: Human tumor cells killed by anthracyclines induce a tumor-specific immune response. *Cancer Res* 71: 4821-4833, 2011.
- Nishio M, Barlesi F, West H, Ball S, Bordoni R, Cobo M, Longeras PD, Goldschmidt J Jr, Novello S, Orlandi F, *et al*: Atezolizumab plus chemotherapy for first-line treatment of nonsquamous NSCLC: Results from the randomized phase 3 IMpower132 trial. *J Thorac Oncol* 16: 653-664, 2021.
- Abbar B, De Castelbajac V, Gougis P, Assoun S, Pluvy J, Tesmoingt C, Théou-Anton N, Cazes A, Namour C, Khalil A, *et al*: Definitions, outcomes, and management of hyperprogression in patients with non-small-cell lung cancer treated with immune checkpoint inhibitors. *Lung Cancer* 152: 109-118, 2021.
- Denis M, Duruisseaux M, Brevet M and Dumontet C: How can immune checkpoint inhibitors cause hyperprogression in solid tumors? *Front Immunol* 11: 492, 2020.
- Li J and Gu J: PD-L1 expression and EGFR status in advanced non-small-cell lung cancer patients receiving PD-1/PD-L1 inhibitors: A meta-analysis. *Future Oncol* 15: 14: 1667-1678, 2019.
- Zhang S, Bai X and Shan F: The progress and confusion of anti-PD1/PD-L1 immunotherapy for patients with advanced non-small cell lung cancer. *Int Immunopharmacol* 80: 106247, 2020.
- Rodríguez-Abreu D, Powell SF, Hochmair MJ, Gadgeel S, Esteban E, Felip E, Speranza G, De Angelis F, Dómine M, Cheng SY, *et al*: Pemetrexed plus platinum with or without pembrolizumab in patients with previously untreated metastatic nonsquamous NSCLC: Protocol-specified final analysis from KEYNOTE-189. *Ann Oncol* 32: 881-895, 2021.
- Siddik ZH: Cisplatin: Mode of cytotoxic action and molecular basis of resistance. *Oncogene* 22: 7265-7279, 2003.
- Henriques AC, Ribeiro D, Pedrosa J, Sarmiento B, Silva PMA and Bousbaa H: Mitosis inhibitors in anticancer therapy: When blocking the exit becomes a solution. *Cancer Lett* 440-441: 64-81, 2019.

36. Zhang Y, Chen X, Gueydan C and Han J: Plasma membrane changes during programmed cell deaths. *Cell Res* 28: 9-21, 2018.
37. De Sousa Linhares A, Battin C, Jutz S, Leitner J, Hafner C, Tobias J, Wiedermann U, Kundi M, Zlabinger GJ, Grabmeier-Pfistershammer K and Steinberger P: Therapeutic PD-L1 antibodies are more effective than PD-1 antibodies in blocking PD-1/PD-L1 signaling. *Sci Rep* 9: 11472, 2019.
38. Lee HT, Lee JY, Lim H, Lee SH, Moon YJ, Pyo HJ, Ryu SE, Shin W and Heo YS: Molecular mechanism of PD-1/PD-L1 blockade via anti-PD-L1 antibodies atezolizumab and durvalumab. *Sci Rep* 7: 5532, 2017.
39. Mohiuddin M and Kasahara K: Cisplatin activates the growth inhibitory signaling pathways by enhancing the production of reactive oxygen species in non-small cell lung cancer carrying an EGFR exon 19 deletion. *Cancer Genomics Proteomics* 18 (3 Suppl): S471-S486, 2021.
40. Marín-Jiménez JA, Capasso A, Lewis MS, Bagby SM, Hartman SJ, Shulman J, Navarro NM, Yu H, Rivard CJ, Wang X, *et al*: Testing cancer immunotherapy in a human immune system mouse model: Correlating treatment responses to human chimerism, therapeutic variables and immune cell phenotypes. *Front Immunol* 12: 607282, 2021.



This work is licensed under a Creative Commons Attribution-NonCommercial-NoDerivatives 4.0 International (CC BY-NC-ND 4.0) License.